

Incorporation and optical activation of erbium in silicon using molecular beam epitaxy

R. Serna, Jung H. Shin, M. Lohmeier, E. Vlieg, A. Polman et al.

Citation: *J. Appl. Phys.* **79**, 2658 (1996); doi: 10.1063/1.361136

View online: <http://dx.doi.org/10.1063/1.361136>

View Table of Contents: <http://jap.aip.org/resource/1/JAPIAU/v79/i5>

Published by the [American Institute of Physics](#).

Related Articles

Enhancement of room temperature dislocation-related photoluminescence of electron irradiated silicon
J. Appl. Phys. **113**, 033518 (2013)

Investigation of the thermal charge “trapping-detrapping” in silicon nanocrystals: Correlation of the optical properties with complex impedance spectra
Appl. Phys. Lett. **101**, 242108 (2012)

Inhomogeneous linewidth broadening and radiative lifetime dispersion of size dependent direct bandgap radiation in Si quantum dot
AIP Advances **2**, 042162 (2012)

Calibration of the photoluminescence technique for measuring concentrations of shallow dopants in Ge
J. Appl. Phys. **112**, 103701 (2012)

On the origin of inter band gap radiative emission in crystalline silicon
AIP Advances **2**, 042135 (2012)

Additional information on J. Appl. Phys.

Journal Homepage: <http://jap.aip.org/>

Journal Information: http://jap.aip.org/about/about_the_journal

Top downloads: http://jap.aip.org/features/most_downloaded

Information for Authors: <http://jap.aip.org/authors>

ADVERTISEMENT



AIP Advances

Now Indexed in Thomson Reuters Databases

Explore AIP's open access journal:

- Rapid publication
- Article-level metrics
- Post-publication rating and commenting

Incorporation and optical activation of erbium in silicon using molecular beam epitaxy

R. Serna,^{a)} Jung H. Shin, M. Lohmeier,^{b)} E. Vlieg, and A. Polman

FOM—Institute for Atomic and Molecular Physics, Kruislaan 407, 1098 SJ Amsterdam, The Netherlands

P. F. A. Alkemade

DIMES/NF, Faculty of Applied Physics, Delft University of Technology, Lorentzweg 1, 2628 CJ Delft, The Netherlands

(Received 26 July 1995; accepted for publication 23 October 1995)

Erbium is incorporated in crystalline silicon during molecular beam epitaxy on Si(100) at 600 °C, either in vacuum (6×10^{-11} mbar) or in an O₂ ambient (4×10^{-10} mbar). Strong Er segregation takes place during growth in vacuum, and only 23% of the total deposited Er is incorporated in the epitaxial layer. Films grown in an O₂ ambient show no Er segregation, and an Er concentration of 1.5×10^{19} Er/cm³ is incorporated in the crystal. The O content is 4×10^{19} O/cm³. Photoluminescence spectra taken at 10 K show the characteristic intra-4*f* luminescence of Er³⁺ at 1.54 μm for both samples, grown with and without O₂. Differences found in the spectral shape indicate a difference in the local environment (presumably O coordination) of Er for the two cases. The O codoped film shows a 7 times higher Er luminescence peak intensity than the film grown without O. This is due to the higher incorporated Er concentration as well as an increased luminescence efficiency (lifetime without O: 0.33 ms, with O: 1.81 ms). The Er excitation efficiency is lower in the O codoped film than in the O-undoped film, which is attributed to the lower minority carrier lifetime in the O-doped material. Thermal annealing of the O codoped film at 1000 °C increases the excitation efficiency and hence the Er luminescence intensity. © 1996 American Institute of Physics. [S0021-8979(96)04903-2]

I. INTRODUCTION

The optical doping of silicon with erbium has been a very active field of research since its introduction by Ennen *et al.*^{1,2} The erbium ion, when incorporated in Si in the trivalent charge state, shows an intra-4*f* transition at a wavelength of 1.54 μm, which is important in optical communication technology. This emission has been observed both under optical and electrical excitation.^{1,2} The optical doping of erbium is thus an attractive method to obtain efficient light emission from Si, thus finding a solution around the problem of the indirect band gap of this semiconductor. The aim is to study the possibility of fabricating light-emitting diodes, lasers, or optical amplifiers based on silicon.

To obtain efficient luminescence in Si it is first necessary to incorporate high concentrations of Er in the crystal.³ Ion implantation has been extensively used for incorporation of Er in Si.^{1,4–8} Erbium implantation induces amorphization of the Si crystal. During solid phase epitaxy (SPE) of the Er-doped amorphous Si, segregation and trapping take place and up to 10^{20} Er/cm³ can be incorporated in the crystal Si,^{6,7} a concentration well above the equilibrium solubility. Erbium coevaporation during Si molecular beam epitaxy (MBE) offers in principle the opportunity to grow in a direct way thick Er-doped layers eliminating the recrystallization step.

We addressed the kinetics of Er incorporation and its limiting factors during Si MBE in a previous paper.⁹ Strong

Er surface segregation during deposition on Si(100) is observed, which is avoided when introducing an oxygen background pressure during growth. This is a result with further implications, since it has been shown that the addition of oxygen to Er-implanted Si enhances the Er luminescence intensity, and reduces the quenching of the luminescence at elevated temperatures.¹⁰ As a result, room temperature photoluminescence^{5,10–13} and electroluminescence^{14,15} from Er and O codoped Si has been observed.

In this article we will focus on the effect of oxygen on the Er-related luminescence at 10 K of the Er-doped MBE-grown Si films compared to films grown without oxygen. A seven-fold enhancement of the peak luminescence intensity is found for an oxygen concentration of $4 \pm 1 \times 10^{19}$ atoms/cm³. The Er active concentration, excitation efficiency, and luminescence efficiency are studied. All these parameters are strongly affected by the presence of oxygen.

II. EXPERIMENT

Erbium-doped epitaxial Si layers were grown in a MBE apparatus utilizing an electron beam evaporator for Si and a Knudsen cell for coevaporation of Er. The Si flux was 1.5×10^{14} atoms/cm² s, and the Er flux 3.1×10^{10} atoms/cm² s. Float-zone Si(100) (*p*-type, 0.17–0.23 Ω cm) wafers were used as substrates. The native oxide on the Si surface was removed by briefly heating the substrates to 1100 °C in ultrahigh vacuum (base pressure of 3×10^{-11} mbar). After this treatment the surface exhibited a clear 2×1 reflection high-energy electron diffraction pattern. A 20-nm-thick Si buffer layer was first grown before opening the Er Knudsen cell to ensure good initial epitaxy. Subsequently,

^{a)}Present address: Instituto de Optica, CSIC, Serrano 121, 28006 Madrid, Spain; Electronic mail: rserna@pinar1.csic.es

^{b)}Present address: Philips Research Laboratories, P.O. Box 80000, 5600 JA Eindhoven, The Netherlands.

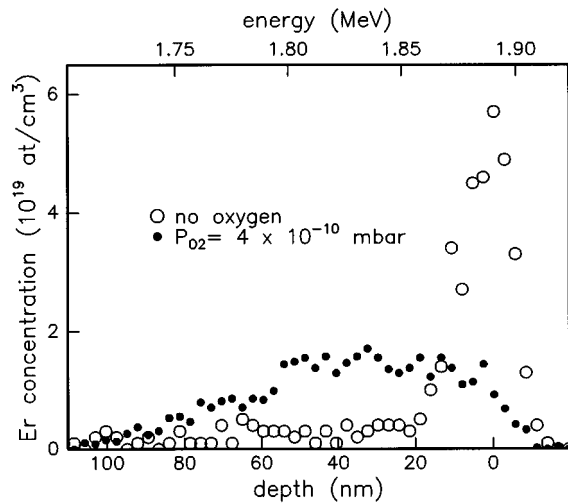


FIG. 1. Er concentration depth profiles for Er-doped MBE Si films grown on Si(100) at 600 °C, without oxygen, and at an oxygen background pressure of 4×10^{-10} mbar.

codeposition of Er and Si was performed, resulting in an ≈ 100 -nm-thick Er-doped film. The typical growth pressure during deposition was 6×10^{-11} mbar, and the substrate temperature was kept at 600 °C. The oxygen pressure in the MBE chamber was controlled through a needle valve.

After growth, a part of each film was annealed in a rapid thermal annealing furnace at 1000 °C under flowing N_2 for 15 s. The Er concentration depth profiles, layer thickness, and Si crystal quality were measured with Rutherford backscattering spectrometry (RBS)/channeling using 2 MeV He. A scattering angle of 100 °C was used to give a depth resolution of 10 nm. The O and Er content of the films after growth was determined with secondary ion mass spectrometry (SIMS) in ultrahigh vacuum using 16 keV Cs^+ sputtering. Secondary ion intensities were converted to atomic densities using known relative sensitivity factors.¹⁶

Photoluminescence (PL) spectroscopy was performed using the 514.5 line of an Ar laser as a pump source. The $1/e$ penetration depth at this wavelength is 890 nm in crystalline Si. The pump power at the sample was varied in the range of 1–150 mW. The spot diameter on the sample was about 2 mm. The pump beam was chopped with an acousto-optical modulator at 23 Hz. The luminescence signal was collected using a 48 cm monochromator, a liquid-nitrogen-cooled Ge detector, and a lock-in amplifier. All PL measurements were performed using a variable temperature closed-cycle helium refrigerator cryostat, with the samples kept in vacuum (10^{-6} mbar). PL decay signals were recorded and averaged using a digitizing oscilloscope system.

III. RESULTS AND DISCUSSION

A. Er incorporation during Si MBE

Figure 1 shows the Er concentration depth profiles of MBE films grown without oxygen (base pressure of better than 6×10^{-11} mbar), and with an oxygen background pressure of 4×10^{-10} mbar. The profiles are obtained from RBS spectra measured in random conditions. The Er spectra mea-

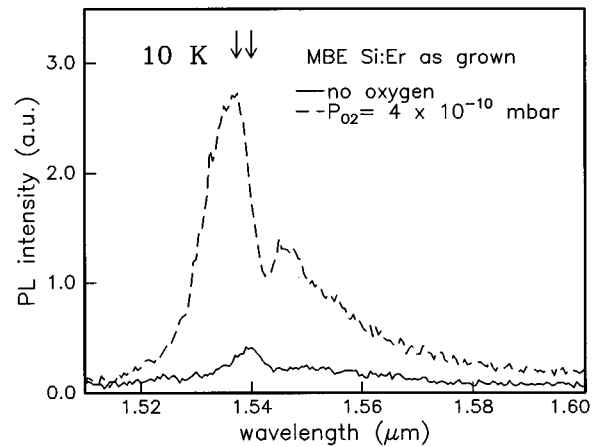


FIG. 2. PL spectra taken at 10 K for Er-doped MBE Si films grown on Si(100) at 600 °C, without oxygen, and at an oxygen background pressure of 4×10^{-10} mbar. The pump power at 514.5 nm was 30 mW; the resolution is 1.5 nm. The arrows indicate the peak wavelength for each spectrum.

sured in channeling conditions (not shown) are identical to those for the random ones, indicating that in both cases Er is not in lattice positions, nor in tetrahedral interstitial sites.⁹ The minimum yield in the Si part of the spectra (not shown) is $\chi_{\min} < 3\%$, indicating good crystal quality.⁹ From the profiles in Fig. 1 it is seen that a clear Er surface peak is observed for the film grown without oxygen background, showing that strong surface segregation takes place during growth, and only a maximum concentration of 4×10^{18} Er/cm³ is incorporated in the crystal. In contrast, the profile for the sample grown in the presence of oxygen shows no segregation, and a trapped Er concentration of 1.5×10^{19} /cm³. The same behavior was found for samples grown at different oxygen pressures in the range of 4×10^{-10} – 2×10^{-9} mbar. It is important to note that in the film grown without oxygen only 23% of the deposited Er is incorporated into the crystal, while in the other films 100% is incorporated.

SIMS measurements for the film grown at 4×10^{-10} mbar oxygen background pressure show an O content in the film of $(4 \pm 1) \times 10^{19}$ O/cm³. The oxygen concentration for the films grown without oxygen is expected to be below 10^{18} O/cm³.

The absence of segregation in the presence of oxygen was discussed in a previous paper.⁹ It has been suggested that O may react with Er at the Si surface forming complexes which can be more easily incorporated than Er alone. Note that O also reduces Er segregation at a moving crystal amorphous interface during Si SPE,^{7,8} indicating that the presence of O increases the effective solubility of Er in crystal Si.¹⁷ In the present article PL measurements will be used to show further evidence of the existence of such complexes.

B. Optical activation of Er in Si grown by MBE

1. PL spectra

Figure 2 shows the Er-related PL spectra at 10 K of the films grown without O, or in an O_2 pressure of 4×10^{-10}

mbar. The spectral resolution is 1.5 nm. In both cases the spectrum shows a clear peak around 1.54 μm , characteristic of transitions between the $^4I_{13/2}$ and $^4I_{15/2}$ manifolds in Er^{3+} . The O-doped films shows a 7 times higher peak intensity and a 4.4 times higher integrated luminescence intensity than the one grown without oxygen. The shape of the luminescence spectra is quite different. For the O-doped film the peak is shifted toward lower wavelength. The side peak at 1.547 μm observed in the O-doped sample is not seen in the pure sample. As the luminescence spectrum is a sensitive probe of the local environment of the Er ion, these data show that the presence of O changes the local structure around the Er,^{5,8,18} presumably by the formation of Er–O complexes.

In order to further analyze the PL data it must be realized that the excitation of Er in Si is through a photocarrier mediated process, i.e., Er is excited electrically, and not by direct optical absorption. This fact has been shown for Er-doped Czochralski-Si (Cz-Si),^{5,17} as well as for heavily oxygen doped Si.^{11–13} Taking this into account, the increase in luminescence intensity of the O-doped film can be due to the following factors.

(1) *The Er concentration incorporated in the crystal is higher.* Indeed, the data in Fig. 1 show that 4 times more Er is incorporated in the O-doped film, due to the absence of Er segregation.

(2) *The fraction of optically active Er ions is higher.* Indeed, it has been suggested that O increases the density of optically active Er ions.^{4,5,17}

(3) *The luminescence efficiency (lifetime) is higher.* The luminescence efficiency is defined as the ratio between radiative and total (radiative plus nonradiative) decay rates of the excited Er ions. Modification of the Er local environment may influence the efficiency of nonradiative energy transfer processes and thereby the luminescence efficiency.¹²

(4) *The Er is more efficiently excited.* For example an increase of the electrical carrier lifetime will lead to a more efficient excitation of Er, and hence to a higher quantum efficiency (defined as the fraction of photogenerated electron–hole pairs that recombine by transferring energy to an Er ion). The coupling from the Si electronic system to the Er-intra 4*f* shell may also be affected by the presence of O.^{18–20}

In the following sections measurements of luminescence lifetime, as well as the pump power dependence of the luminescence will allow us to study and discuss issues (2), (3), and (4), while issue (1) was already discussed above.

2. Luminescence efficiency (lifetime)

Figure 3 shows normalized luminescence decay traces at 1.54 μm for the samples grown in presence of 4×10^{-10} mbar O_2 and without O_2 , measured at 10 K. The $1/e$ time values are 1.81 and 0.33 ms for the films grown with and without oxygen, respectively. The decay traces show no significant change when the temperature is increased up to 100 K. This result is the first report for a lifetime over 1 ms in Er-doped Si.^{10,17} The increase in luminescence intensity for the O-doped sample (Fig. 2) is partially due to this five fold enhancement of the luminescence efficiency. It must be noted that Si:Er films codoped with oxygen by ion implan-

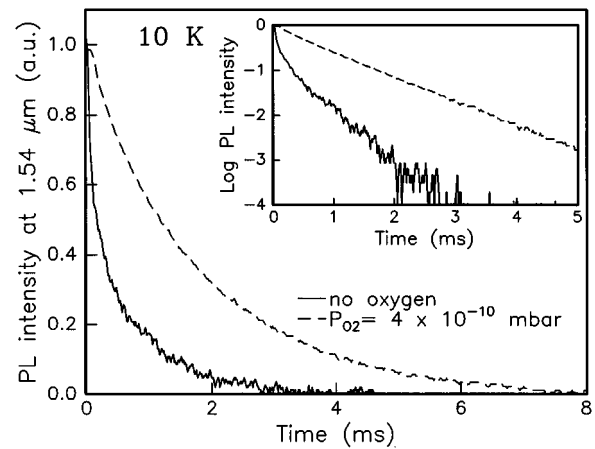


FIG. 3. Normalized time decay of the 1.54 μm luminescence taken at 10 K for Er-doped MBE Si films grown on Si(100) at 600 $^{\circ}\text{C}$, without oxygen, and at an oxygen background pressure of 4×10^{-10} mbar. The inset shows the data on a logarithmic scale. The pump power at 514.5 nm was 60 mW. The spectral resolution was set to 10 nm.

tation have always shown lifetimes well below 1 ms even at temperatures as low as 77 K.^{10,12} Further differences with ion-implanted samples can be seen in the inset of Fig. 3 in which the luminescence decay traces at 10 K are shown on a logarithmic scale. The decay trace for the O-doped sample shows a nearly single exponential behavior characterized by a time constant of 2 ms, whereas the O-undoped film shows a clear double exponential decay characterized by a fast decay of 80 μs followed by a slower decay of 0.9 ms. Measurements performed in ion-implanted samples at 77 K showed double-exponential decay races both for O-undoped and O-doped samples. The high luminescence lifetimes found for the MBE O-doped samples indicate that nonradiative luminescence quenching processes in O-doped Si:Er films are less efficient in MBE-grown films than in ion-implanted films, at least at 77 K.

3. Er active fraction and excitation efficiency

In order to determine the relative fraction of active Er ions in the films, as well as the excitation efficiency, measurements of the dependence of the 1.54 μm luminescence intensity on the excitation power were performed for both films. Figure 4 shows the luminescence peak intensity for each film measured as function of the excitation power. As the spectral resolution was set to 10 nm, an integrated intensity measurement is obtained over this wavelength range. For low powers the luminescence intensity increases with power, while saturation is observed for the highest pump powers used.

To interpret these data it can be assumed that the luminescence intensity is proportional to $n_{\text{Er}} w_{\text{rad}}$, with n_{Er} the areal density of excited ions and w_{rad} the radiative decay rate which we assume to be the same for both samples. The rate equation for n_{Er} can be written as

$$\frac{dn_{\text{Er}}}{dt} = PQ(n_o - n_{\text{Er}}) - \frac{n_{\text{Er}}}{\tau}, \quad (1)$$

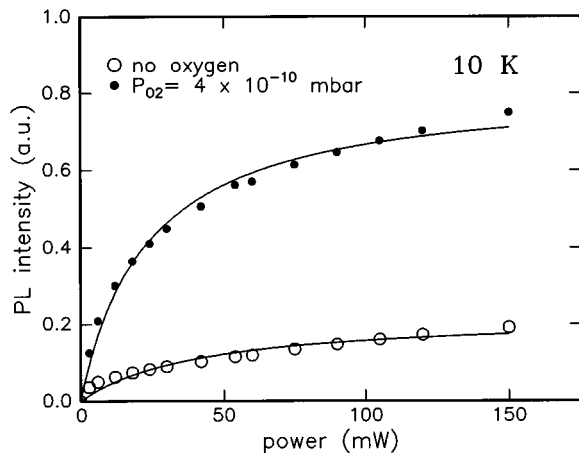


FIG. 4. Peak value of the PL intensity as a function of pump power taken at 10 K for Er-doped MBE Si films grown on Si(100) at 600 °C, without oxygen, and at an oxygen background pressure of 4×10^{-10} mbar. The spectral resolution was set to 10 nm. The solid line is a fit of Eq. (2) to the experimental data.

where P is the excitation power, Q is a factor which includes the quantum efficiency of the process (which is dependent on the temperature and excitation wavelength, as well as on geometrical factors), n_o is the areal density of optically active Er ions, and τ is the luminescence lifetime.

In equilibrium $dn_{\text{Er}}/dt = 0$ so that

$$n_{\text{Er}} = \frac{n_o}{1 + \frac{P}{PQ\tau}} \quad (2)$$

Note that for high excitation power ($P \gg 1/Q\tau$) $n_{\text{Er}} \approx n_o$, while for low excitation powers ($P \ll 1/Q\tau$) the excited Er concentration is linear with power: $n_{\text{Er}} \approx PQn_o\tau$. The best fit to Eq. (2) is overlaid with the experimental data in Fig. 4. The fit parameters n_o and Q together with the measured $1/e$ lifetimes (τ) from Fig. 3 are listed in Table I. Since the luminescence intensity is given in arbitrary units, the values for n_o and Q are only relative values, and will be used to establish a comparison between the two films. In Table I the values for n_o and Q are normalized to the values for the sample grown without O_2 . The data for n_o show that the O-doped film has a 3.7-fold higher density of active Er ions than the film grown without oxygen. Note that the total amount of Er incorporated in the O-doped film is also 4 times higher than that in the film grown without oxygen (see

TABLE I. Lifetime (τ), relative number of optically/active Er ions (n_o), and relative quantum efficiency (Q) for the films grown without oxygen, and at oxygen background pressure of 4×10^{-10} mbar. The total trapped Er areal density is also indicated. The values of n_o , and Q are obtained using Eq. (2) to fit luminescence power dependence measurements (Fig. 4), and are normalized to the values for the sample grown without oxygen.

P_{O_2} (mbar)	Er/cm ²	τ (ms)	n_o	Q
No oxygen	3×10^{13}	0.33	1	1
4×10^{-10}	1×10^{14}	1.81	3.7	0.35
4×10^{-10} ^a	1×10^{14}	1.68	6.6	0.48

^aAnnealed.

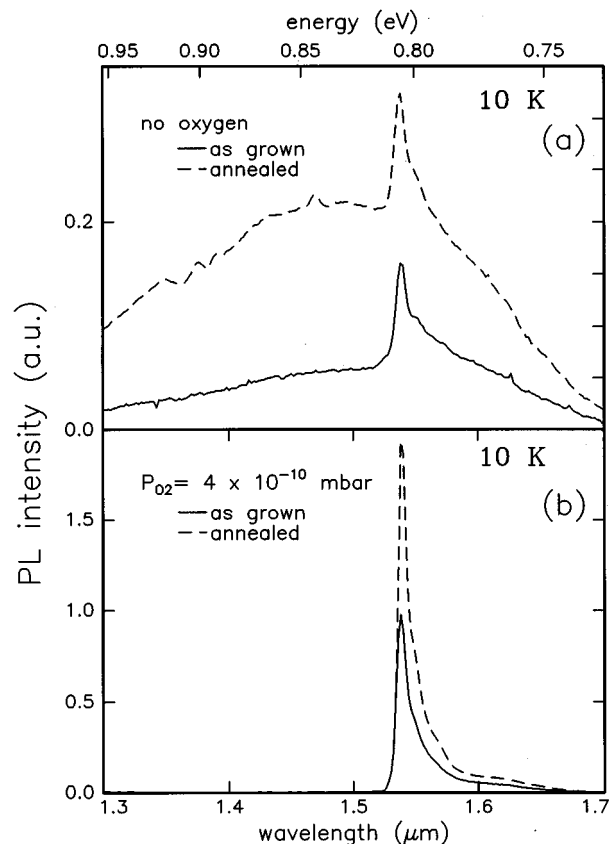


FIG. 5. PL spectra taken at 10 K for Er-doped MBE Si films grown on Si(100) at 600 °C, as grown and after an annealing at 1000 °C 15 s, without oxygen (a), and at an oxygen background pressure of 4×10^{-10} mbar (b). The pump power at 514.5 nm was 60 mW; the resolution is 6 nm.

Fig. 1). We therefore conclude that the Er optically active fraction is not modified by the presence of oxygen.

The 3-times lower Q value obtained for the O-doped film reflects a lower excitation efficiency. This may be due to structural defects in the Si crystal related to the O incorporation, which cause a reduction in the electrical carrier lifetime. Since Er excitation in Si takes place via photogenerated carriers, this results in a less efficient Er excitation.

Altogether the increase in PL intensity for the O-doped sample over the whole range of pump powers used is attributed to the combined effect of: a 3.7 times more active Er fraction (a fourfold increase in incorporated Er), a 5.4 times higher luminescence efficiency, and a factor of 0.35 lower excitation efficiency. It must be noted that these results hold at 10 K, and can be extended up to 100 K, but they cannot be extrapolated at temperatures close to room temperature where the situation is likely to be strongly modified, as has been shown in Er ion implanted films.¹⁰

4. Annealing behavior

In order to study a possible improvement of the luminescence characteristics, after deposition a part of each film was annealed at 1000 °C for 15 s. This procedure is shown to lead to optimum luminescence in Er-implanted Si.¹⁷ Figure 5 shows the PL spectra for samples grown with and without oxygen before and after the anneal. A broad luminescence

band between 1.3 and 1.7 μm is seen in the as-grown film without oxygen [Fig. 5(a)], superimposed on the characteristic Er luminescence. The broad luminescence band increases further upon annealing, while the Er-related luminescence is, essentially, not modified by the annealing. The broad band has been observed in all the films grown without oxygen, including samples grown on Si(111) substrates.⁹ It may be related to defects and strain in the Si crystal or to the formation of erbium silicide precipitates at the surface of the film. The absence of the defect band in the O-doped films [Fig. 5(b)] may be related to the absence of Er-related defects and precipitates.

Thermal annealing increases the PL peak luminescence for the O-doped film by a factor of 2. The same behavior is observed for other films grown under different oxygen pressures in the range of 4×10^{-10} – 2×10^{-9} mbar. The analysis of the luminescence dependence on the power excitation using Eq. (2) has been performed for the annealed O-doped film as well. No analysis is done for the film grown without oxygen since the luminescence is dominated by the broad defect-related luminescence band. The values obtained for τ , n_o , and Q for the annealed O-doped film are included in Table I. After annealing the fraction of excitable Er ions is increased almost twofold. The excitation efficiency is increased as well, probably due to a reduction of the density of carrier recombination centers upon annealing. The measured Er luminescence lifetime is only slightly modified, indicating that annealing does not lead to a substantial change in the Er local environment.

The behavior observed upon annealing in our MBE grown films can be very well correlated with that found for Er-implanted float-zone grown (FZ) Si (O concentration $< 10^{16}/\text{cm}^3$) and Cz-Si (O concentration $\approx 10^{18}/\text{cm}^3$). Annealing of Cz-Si leads to an increase of the luminescence intensity, while in FZ-Si even a decrease is observed.⁵ In the present experiment annealing of the O-doped sample also leads to an increased PL intensity [Fig. 5(b)] while Er luminescence in the O-undoped sample shows no change on annealing. In implanted Cz-Si the increase in luminescence intensity after annealing has been attributed to annealing of carrier recombination centers.¹⁷ Quite similarly, our O-doped films show an increased excitation efficiency (see the Q value in Table I).

IV. CONCLUSIONS

In conclusion, we have studied the incorporation and optical activation of Er in Si using MBE. Er segregation takes place during Si MBE; it can be avoided when a low oxygen pressure (4×10^{-10} mbar) is present during growth. As-grown films with or without oxygen both show characteristic Er^{3+} luminescence at 1.54 μm at 10 K, but with different spectral shapes. This is attributed to the fact that Er forms microscopic clusters with oxygen. The O-doped film

shows a higher luminescence intensity than the O-undoped film due to the fact that a larger Er concentration is trapped in the crystal, and because the O-doped film shows a higher Er luminescence efficiency (longer lifetime). The Er excitation efficiency is lower in the O-doped films than in the O-undoped film, presumably because the presence of O lowers the minority carrier lifetime. Thermal annealing of the O-doped film at 1000 °C increases the excitation efficiency and hence the luminescence intensity.

ACKNOWLEDGMENTS

This work is part of the research program of the Foundation for Fundamental Research on Matter (FOM) and was made possible by financial support from the Dutch Organization for the Advancement of Pure Research (NWO), the Netherlands Technology Foundation (STW), and the IC Technology Program (IOP Electro-Optics) of the Ministry of Economic Affairs. R.S. acknowledges financial support from CSIC, Spain.

- ¹H. Ennen, J. Schneider, G. Pomrenke, and A. Axman, *Appl. Phys. Lett.* **43**, 943 (1983).
- ²H. Ennen, G. Pomrenke, A. Axman, K. Eisele, W. Haydl, and J. Schneider, *Appl. Phys. Lett.* **46**, 381 (1985).
- ³Y. H. Xie, E. A. Fitzgerald, and Y. J. Mii, *J. Appl. Phys.* **70**, 3223 (1991).
- ⁴P. N. Favenec, H. L'Haridon, D. Moutonnet, M. Salvi, and M. Gauneau, *Jpn. J. Appl. Phys.* **29**, L521 (1990).
- ⁵J. Michel, J. L. Benton, R. F. Ferrante, D. C. Jacobson, D. J. Eaglesham, E. A. Fitzgerald, Y. -H. Xie, J. M. Poate, and L. C. Kimerling, *J. Appl. Phys.* **70**, 2672 (1991).
- ⁶A. Polman, J. S. Custer, E. Snoeks, and G. N. van den Hoven, *Appl. Phys. Lett.* **62**, 507 (1993).
- ⁷J. S. Custer, A. Polman, and H. M. van Pinxteren, *J. Appl. Phys.* **75**, 2809 (1994).
- ⁸F. Priolo, S. Coffa, G. Franzó, C. Spinella, A. Carnera, and V. Bellani, *J. Appl. Phys.* **74**, 4936 (1993).
- ⁹R. Serna, M. Lohmeier, P. M. Zagwijn, E. Vlieg, and A. Polman, *Appl. Phys. Lett.* **66**, 1385 (1995).
- ¹⁰S. Coffa, G. Franzó, F. Priolo, A. Polman, and R. Serna, *Phys. Rev. B* **49**, 16313 (1994).
- ¹¹S. Lombardo, S. U. Campisano, G. N. van den Hoven, A. Cacciato, and A. Polman, *Appl. Phys. Lett.* **63**, 1942 (1993).
- ¹²G. N. van den Hoven, A. Polman, S. Lombardo, and S. U. Campisano, *J. Appl. Phys.* **78**, 2642 (1995).
- ¹³R. Serna, E. Snoeks, G. N. van den Hoven, and A. Polman, *J. Appl. Phys.* **75**, 2644 (1994).
- ¹⁴G. Franzó, F. Priolo, S. Coffa, A. Polman, and A. Carnera, *Appl. Phys. Lett.* **64**, 2235 (1994).
- ¹⁵S. Lombardo, S. U. Campisano, G. N. van den Hoven, and A. Polman, *Nucl. Instrum. Methods B* **96**, 378 (1995).
- ¹⁶R. G. Wilson, F. A. Stevie, and C. W. Magee, *Secondary Ion Mass Spectrometry* (Wiley, New York, 1989).
- ¹⁷A. Polman, G. N. van den Hoven, J. S. Custer, J. H. Shin, R. Serna, and P. F. A. Alkemade, *J. Appl. Phys.* **77**, 1256 (1995).
- ¹⁸F. Priolo, G. Franzó, S. Coffa, A. Polman, S. Libertino, R. Barklie, and D. Carey, *J. Appl. Phys.* **78**, 3874 (1995).
- ¹⁹S. Libertino, S. Coffa, G. Franzó, and F. Priolo, *J. Appl. Phys.* **78**, 3867 (1995).
- ²⁰Jung H. Shin, G. N. van den Hoven, and A. Polman, *Appl. Phys. Lett.* **67**, 377 (1995).